Christian Pluchar
Mentor: Keita Kawabe
LIGO SURF 2017 First Interim Report

Introduction

The Advanced LIGO detectors are four kilometer Michelson interferometers. Improvements to the detectors have resulted in multiple detections of gravitational waves from binary black hole mergers. Additional improvements to lower noise from terrestrial and detector sources and progress towards the Advanced LIGO design sensitivity will allow for a larger signal to noise ratio in the detector. The interferometer measures the change in distance between two test masses relative to each other. Through a series of additional optical features designed to increase the effective beam length, kilowatts of laser power are present in the beam cavities during operation, and despite the precision of the mirrored surface of each of the test masses, some light scatters off the test masses and out of the beam path [1]. DSLR cameras have been installed at the LIGO Hanford Observatory in order to observe this scattering. Detector sensitivity increases as the power circulating in the beam cavity increases [1], so minimizing scattering off of the test masses will lead to better performance. While the images are useful in order to qualitatively observe the scattering, in order to measure the amount of energy scattered off the test masses, the cameras must be calibrated to equate the sensor output to the corresponding energy which was incident on the sensor. This project is a continuation of a project started by a SURF student in 2016 (Chen Jie Xin).

Methods

My primary work so far has been to calibrate the camera which faces the end test mass (a Nikon D7100). The camera is placed out of the beam path and directed at the mirror so that it can observe a fraction of the scattered light off the mirror.

Modern digital cameras contain sensors which are covered with photosensitive semiconducting material. Each sensor contains thousands of individual photosensitive sites which correspond to pixels. Each photosite on the camera actually contains four separate elements. For the camera used in this work, one element is primarily sensitive to red light, one primarily sensitive to blue light, and two primarily sensitive to green light [2]. Each of these elements produce a current which is linearly proportional to the amount of light which is incident on the element [3]. The camera then records this data and turns it into an image. While the sensors are designed to be sensitive primarily to visible light, they are also sensitive to infrared wavelengths, including the wavelengths used by the main laser in the aLIGO detectors (1064nm) [4]. The camera was set to record the sensor data as a RAW image. RAW file formats preserve the unaltered sensor data, including the sensor counts of each of the four individual elements of each pixel in addition to leaving the images uncompressed. Other formats (such as JPEG) have a number of processes applied (white balance, demosaicing, compression) to them in order to produce appealing photographs (properly bright, smooth edges, small image file size) [3]. However, these processes can alter the linear proportionality between the amount of light incident on the sensor and the resulting count produced by the elements of the sensor. For this project, the linear proportionality of the pixel count on the number of photons incident on the images sensor is important because the pixel count will also be proportional to the power incident on the sensor. The calibration therefore relates the count output of the sensor to the amount of energy incident on the sensor for a particular wavelength of light.

To measure the calibration, images were recorded in a dark room with the laser light incident directly incident on the camera sensor. The power of the laser was measured using a photodiode power sensor. The images were recorded at a variety of shutter speeds and the laser power was adjusted in order to vary the energy incident on the sensor. The ISO of the camera was kept constant. The camera distance from the laser was varied over different trials so the effect of the beam profile on the calibration could be measured. A conscious effort was made to keep the images from saturating, which could alter the calibration. A series of images was also taken with the laser completely off to measure the background light of the room. The images were then run through a Python script which took a group of RAW image files and computed the total number of counts for each for the red, green, and blue photosites.

Results

The initial issue addressed was the apparent difference in calibration between different beam profiles in previous testing [5]. Light scattering off of the test mass has its own unique profile. In order to appropriately apply the calibration to finding the power of the scattered light off the test masses, which have their own unique profile, it must be verified that the calibration is independent of the beam profile.

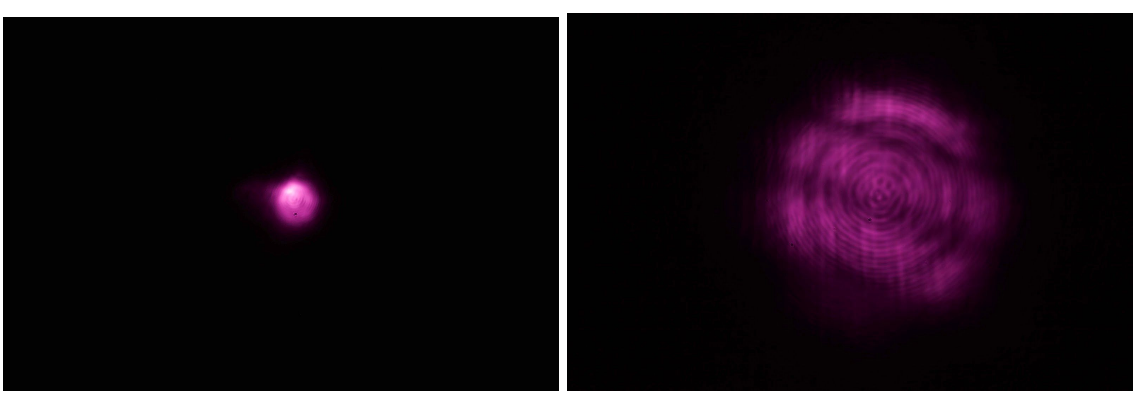

Figure 1: Sample images showing the narrow (left) and wide (right) beam profiles used in the 980nm calibration.

In previous testing, the calibration of the camera depended on the beam profile. In my testing however, the counts of each of the photosites in the camera have been shown to be linear with the energy incident on them, and the counts have also been shown to be independent of beam size.

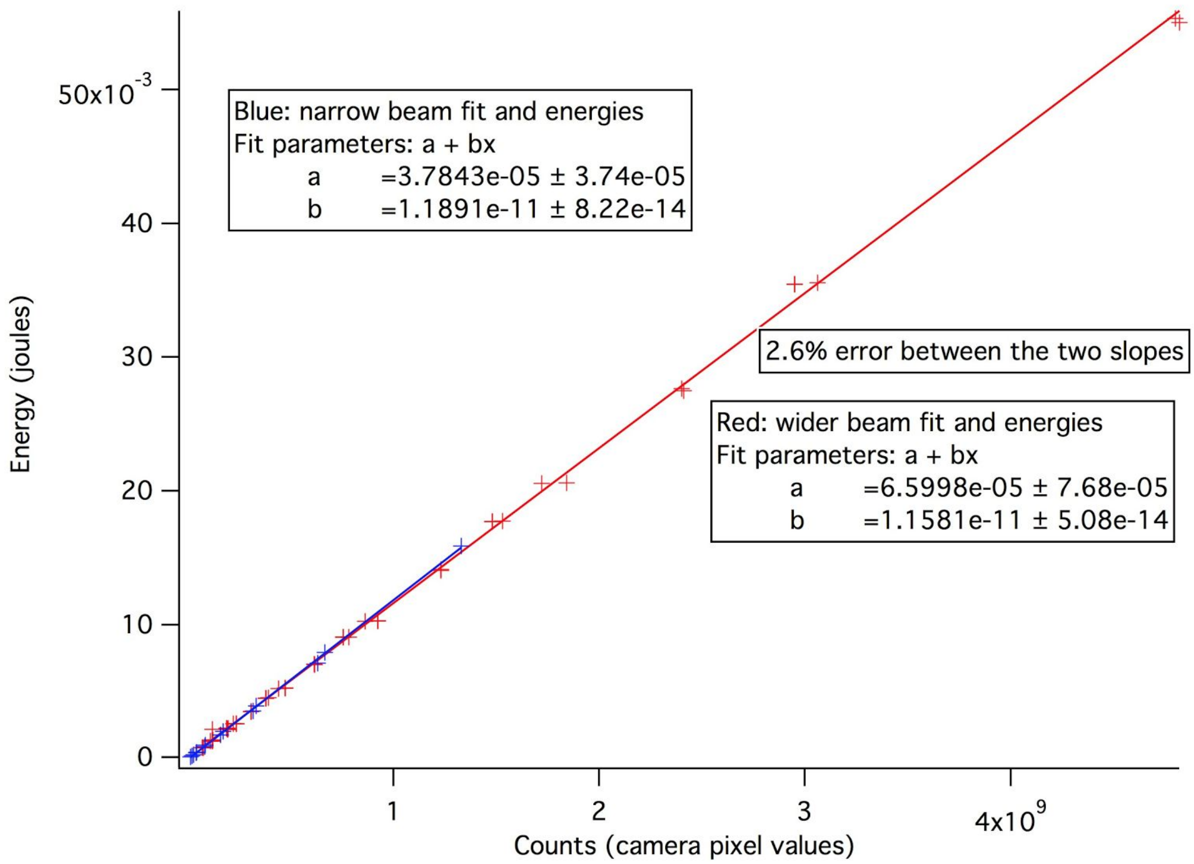

Figure 2: Beam profile comparison for the 980nm laser. The slopes of the lines represent the conversions between the sensor output (counts) and the energy incident on the sensor.

My first set of data to calibrate the Nikon D7100 was performed using a 980nm laser. However, the laser used in the aLIGO detectors are 1064nm. The calibration was then performed again with the new laser wavelength. The calibration here showed again that the counts were linearly dependent on energy and independent of beam size.

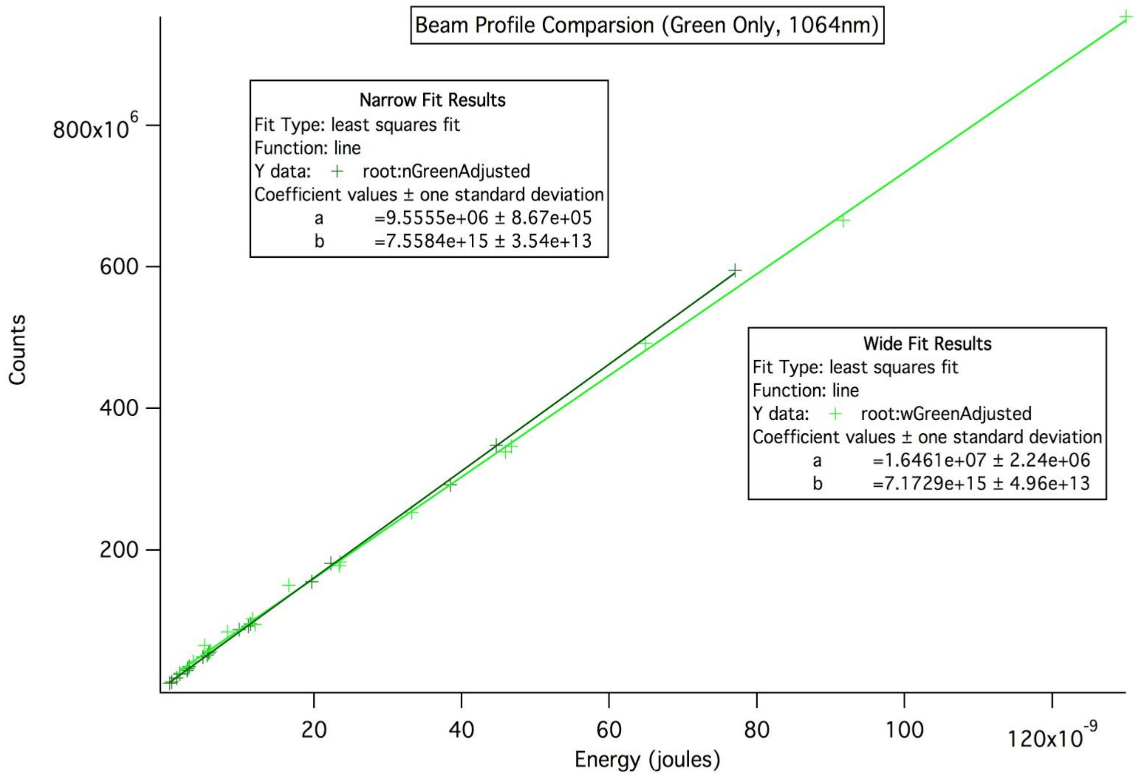

Figure 3: Beam profile comparison for 1064nm laser. Green has only been shown here.

After confirming the calibration is independent of beam size, the calibration for each colored photosite were calculated. The following analysis made the simplifying assumption that one quarter of the laser power was incident on the red and blue photosites, and half the power was incident on the green photosites.

Color	Slope (Counts/Joule)	Standard Deviation
Red	1.61E+16	9.32E+13
Green	1.45E+16	8.26E+13
Blue	1.65E+16	9.52E+13

Table 1: 1064nm Calibration Results. A linear fit was performed on all of the data collected with the 1064nm laser, and the calibration (in counts/joule) were found for the red, green, and blue channels.

To complete the preceding analysis, a Python script was developed to analyze groups of images. The script extracts data from the separate red, green, and blue color sensors on the camera's sensor from each RAW image file using a Python package called Rawpy. It can be setup to average the counts from a group of similar images, and then export that data to a text file. It also has a check to ensure the pixels are not overexposed (which could introduce an error in the calibration), and notifies the user if any overexposed (saturated) pixels are found.

Investigations into why the previous calibration achieved this result were inconclusive. One set of images set of images appeared to match the calibration of the new results down to a factor of two (which can likely be attributed to the difference in ISO settings used), but the other set of images deviated more substantially.

Further Work

In the coming days, I hope to start to analyze the images of the scattering off the test mass and determining how much energy is contained in individual features in the image, or an estimate of the scattering off the test mass as a whole. Additionally, there are two models of cameras installed to observe the scattering. I am planning in the near future to calibrate this camera model as well.

References

1. B. P. Abbott, et al., GW150914: The Advanced LIGO detectors in the era of first discoveries, Physical Review Letters, 116, 131103 (2016).
2. Digital Camera Sensors, WWW Document, (http://www.cambridgeincolour.com/tutorials/ camera-sensors.htm).
3. Understanding Digital Raw Capture, WWW Document, (https://www.adobe.com/digitalimag/pdfs/understanding_digitalrawcapture.pdf).
4. LIGO’s Laser, WWW Document, (https://www.ligo.caltech.edu/page/laser).
5. Chen Jie Xin, Development of optical imaging system for LIGO test mass contamination and beam position monitoring, LIGO Document Control Center, (https://dcc.ligo.org/DocDB/0128/T1600390/002/ligo_final_report.pdf).